ARTICLES
PUBLISHED ONLINE: 6 JUNE 2010 | DOI: 10.1038/NCHEM.700
nature chemistry

Reversible dioxygen binding in solvent-free liquid myoglobin

Adam W. Perriman[1], Alex P. S. Brogan[1], Helmut Cölfen[2†], Nikolaos Tsoureas[3], Gareth R. Owen[3] and Stephen Mann[1]*

The ensemble of forces that stabilize protein structure and facilitate biological function are intimately linked with the ubiquitous aqueous environment of living systems. As a consequence, biomolecular activity is highly sensitive to the interplay of solvent–protein interactions, and deviation from the native conditions, for example by exposure to increased thermal energy or severe dehydration, results in denaturation and subsequent loss of function. Although certain enzymes can be extracted into non-aqueous solvents without significant loss of activity, there are no known examples of solvent-less (molten) liquids of functional metalloproteins. Here we describe the synthesis and properties of room-temperature solvent-free myoglobin liquids with near-native structure and reversible dioxygen binding ability equivalent to the haem protein under physiological conditions. The realization of room-temperature solvent-free myoglobin liquids with retained function presents novel challenges to existing theories on the role of solvent molecules in structural biology, and should offer new opportunities in protein-based nanoscience and bionanotechnology.

It has been widely accepted that the intra- and intermolecular forces that arise from the presence of water molecules are essential for protein structure and function. For example, numerous examples of enzymes that retain their native structure and catalytic activity in non-aqueous media have been reported[1–9], and although these solvents contained no bulk water, the presence of strong intramolecular hydrogen bonds and surface-bound water molecules enclosed in a nonpolar solvent sheath was sufficient to stabilize protein structure and function[10]. However, recent studies using electrospray ionization mass spectrometry have shown that in bovine β-lactoglobulin protein–ligand interactions, the nature of the active site is preserved inside dry vacuum, suggesting that the degree to which water molecules stabilize protein structures may be overstated[11].

In earlier work we reported the formation of the first solvent-free liquid protein, which was produced by room-temperature melting of a freeze-dried nanoconstruct prepared by surface modification of the large, structurally robust iron-storage protein ferritin[12]. The nanoconstruct was formed as a single-component, stoichiometric conjugate by electrostatic grafting of an anionic polymer surfactant with a central polyethylene glycol moiety to surface-accessible cationized amino-acid residues. The corresponding increase in the range of intermolecular attractive interactions was sufficient to facilitate melting of the dry surface-modified protein to produce a solvent-free protein liquid with interesting temperature-dependent rheological properties. These melts can be considered to be a novel type of ionic liquid in which the cationic component is of nanoscale dimension.

Although ferritin has an inherent ability to sequester and assemble inorganic nanoparticles of varied compositions[13,14], it is structurally and functionally atypical when compared with conventional globular proteins and enzymes, which to date have not been prepared as solvent-free molten liquids, even though many of these macromolecules have important applications in bionanoscience. We have therefore explored the possibility of preparing a new class of solvent-less liquids based on haem proteins that exhibit retention of the globular structure and metallocentre function in the molten state. Specifically, here we show, for the first time, that solvent-less liquids of the dioxygen binding protein myoglobin can be prepared by thermally induced melting of lyophilized samples of protein–polymer surfactant nanoconjugates produced by electrostatic binding of the cationized biomolecules to the anionic polymer surfactants poly(ethylene glycol) 4-nonylphenyl 3-sulfopropyl ether ($\mathbf{S}_1$) or glycolic acid ethoxylate lauryl ether ($\mathbf{S}_2$). The nanoconjugates were initially produced in water as stoichiometric, single-component constructs that were then dehydrated and subsequently melted into the liquid phase in the absence of solvent molecules. Significantly, the myoglobin-derived solvent-less liquids exhibited a high level of structural integrity, and as a consequence remained functionally active within the molten state with respect to binding of O_2, CO or SO_2 to the haem metallocentre.

Reproducible preparation of solvent-free protein liquids of met-myoglobin (Mb) was achieved by using a common strategy comprising a sequence of three key steps (see Supplementary Materials and Methods): (i) covalent linking of *N*,*N*-dimethyl-1,3-propanediamine (DMPA) to prepare protein molecules with high surface positive charge, (ii) electrostatically induced complexation of the cationized protein with the anionic polymer surfactants $\mathbf{S}_1$ (C_9H_{19}–C_6H_4–$(OCH_2CH_2)_n O(CH_2)_3SO_3^-$; $n = 20$) or $\mathbf{S}_2$ (CH_3–$(CH_2)_x$–O–$(CH_2CH_2O)_n CH_2$–COOH; $x = 11$–13, $n = 11$) to produce aqueous solutions of single-component nanoconjugates ([**C**–Mb][$\mathbf{S}_x$] ($\mathbf{S}_x = \mathbf{S}_1, \mathbf{S}_2$), and (iii) lyophilization of the nanoconjugate solutions to afford freeze-dried ionic nanoconstructs that subsequently underwent thermally induced melting at ambient temperatures and pressure to produce translucent dark brown viscous solvent-less liquids that flowed under gravity (Fig. 1). Changing the anionic surfactant headgroup from a sulfonate ($\mathbf{S}_1$) to a carboxylate ($\mathbf{S}_2$) moiety had no observable effect on the viscosity of the liquids. In the case of [**C**–Mb][$\mathbf{S}_2$], reducing the number of polyethylene oxide (PEO) repeat units in the glycolic acid ethoxylate

[1]Centre for Organized Matter Chemistry, School of Chemistry, University of Bristol, Bristol BS8 1TS, UK, [2]Max-Planck-Institute of Colloids and Interfaces, Am Mühlenberg, D-14476 Golm, Germany, [3]School of Chemistry, University of Bristol, Bristol BS8 1TS, UK; †Present address: University of Konstanz, Physical Chemistry, Universitätsstraße 10, D-78464 Konstanz, Germany. *e-mail: S.Mann@bristol.ac.uk

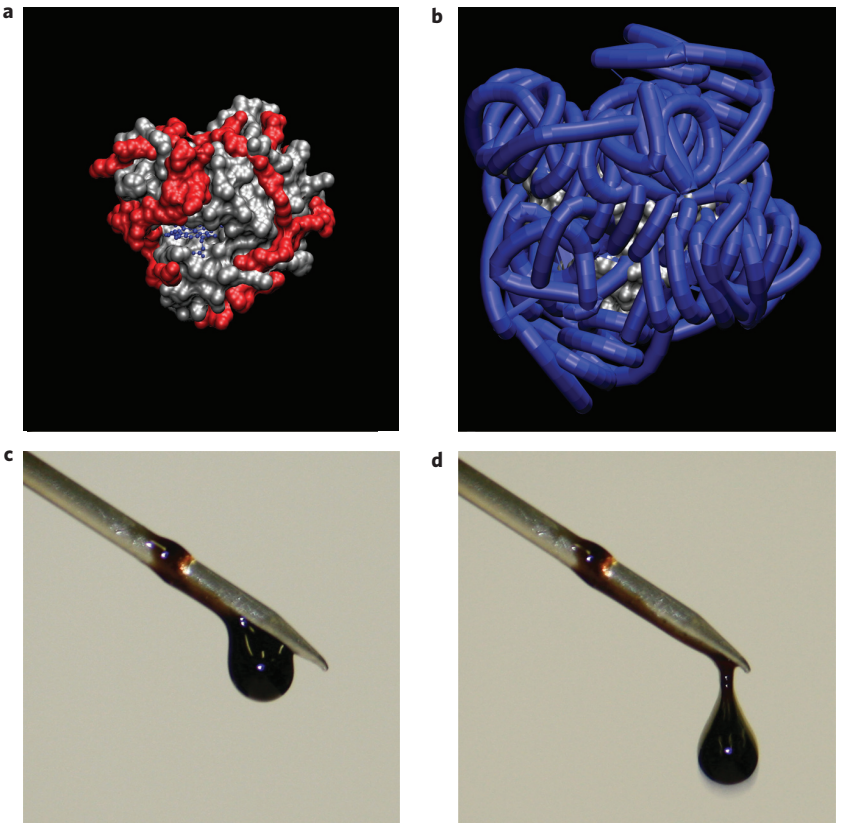

Figure 1 | Solvent-free liquid Mb. a, Solvent accessible surface of Mb, showing a positive surface charge distribution (red) obtained after cationization with covalently linked DMPA. **b**, Graphic depicting electrostatic binding of the anionic polymer surfactant to cationized Mb to produce a surface-modified hybrid nanoconstruct. **c**,**d**, Photographs showing a time sequence of gravity-induced flow of a solvent-free Mb liquid droplet at 60 °C and atmospheric pressure after 5 s (**c**) and 10 s (**d**). The spheroidal shape exhibited by the pendant droplet results from the high surface tension.

lauryl ether from 11 ($\mathbf{S}_2$) to 6 ($\mathbf{S}_3$) resulted in the formation of a tacky deformable solid, with a further reduction to 4 PEO units ($\mathbf{S}_4$) resulting in a complete absence of melting.

Detailed studies were undertaken on the [**C**–Mb][$\mathbf{S}_x$] melts to determine their structural properties and, significantly, to ascertain whether biomolecular functionality was retained in the solvent-free liquid phase. Cationization of met-Mb was readily achieved by carbodiimide-activated coupling to give a complex comprising approximately 17 covalently coupled DMPA moieties (mass spectroscopy data, Supplementary Fig. S1). This was consistent with zeta potential measurements that showed a significant increase in surface charge from −10 mV to +42 mV for the native and cationized protein, respectively. Electrostatic conjugation with $\mathbf{S}_2$ to produce aqueous dispersions of the corresponding ionic nanoconstructs was associated with a concomitant decrease in the zeta potential to +2 mV. Binding of the polymer surfactant $\mathbf{S}_2$ was confirmed by ^{1}H nuclear magnetic resonance (NMR) spectroscopy, which showed an upfield chemical shift of the protons of the α carbon to the carboxylate group from 4.14 ($\mathbf{S}_2$) to 4.00 ppm ([**C**–Mb][$\mathbf{S}_2$]) (Supplementary Fig. S2). Sedimentation coefficient distributions obtained by analytical ultracentrifugation of aqueous solutions of [**C**–Mb][$\mathbf{S}_1$] showed a single peak maximum at 2.1 S, compared with a value of 1.4 S for $\mathbf{S}_1$ alone (Supplementary Fig. S3). The increase in the sedimentation velocity of the conjugate and the absence of free $\mathbf{S}_1$ were consistent with the formation of a discrete protein–polymer surfactant ionic construct. Dynamic light scattering (DLS) measurements also showed unimodal distributions for aqueous solutions of **C**–Mb and [**C**–Mb][$\mathbf{S}_1$], which gave respective hydrodynamic diameters of 3.3 and 4.8 nm (Supplementary Fig. S4).

The above results are consistent with the formation of aqueous dispersions of single-component, electrically neutral, discrete myoglobin–polymer surfactant nanoconjugates. As such, lyophilization of the aqueous [**C**–Mb][$\mathbf{S}_1$] or [**C**–Mb][$\mathbf{S}_2$] constructs produced low-density ionic solids, which, as shown in Fig. 1, melted at room temperature and ambient pressure to produce translucent viscous liquids. Thermogravimetric analysis of the [**C**–Mb][$\mathbf{S}_1$] fluid gave a residual water content of less than 0.1 wt% and a decomposition temperature of 408 °C, which was 93 °C higher than that of the pure lyophilized myoglobin (Supplementary Fig. S5). Although no increase in weight loss was observed when the myoglobin melts were heated to between 100 and 250 °C, the possibility of tightly bound surface water cannot be ruled out. In this regard, using established theory[15,16], we calculated that the number of water molecules associated specifically with anionic and polar amino acids at the native myoglobin surface constituted ~3.4 wt%. An equivalent calculation for the [**C**–Mb][$\mathbf{S}_1$] melt in which the number of water binding sites was reduced stoichiometrically by DMPA cationization and $\mathbf{S}_1$ binding gave a theoretical water content of ~0.3 wt% (four water molecules per protein–polymer surfactant conjugate), which was close to the value determined experimentally.

Significantly, differential scanning calorimetry (DSC) of the lyophilized [**C**–Mb][$\mathbf{S}_1$] construct showed thermal characteristics that deviated substantially from $\mathbf{S}_1$ alone (Fig. 2a). Upon heating from −50 °C, both $\mathbf{S}_1$ and [**C**–Mb][$\mathbf{S}_1$] displayed first-order phase transitions at −14 and −18 °C, respectively, although no crystallization peak was apparent for [**C**–Mb][$\mathbf{S}_1$] on cooling, which suggests a reduction in the rate of reordering in [**C**–Mb][$\mathbf{S}_1$]. In addition, $\mathbf{S}_1$ showed a large endothermic melting transition consisting of a

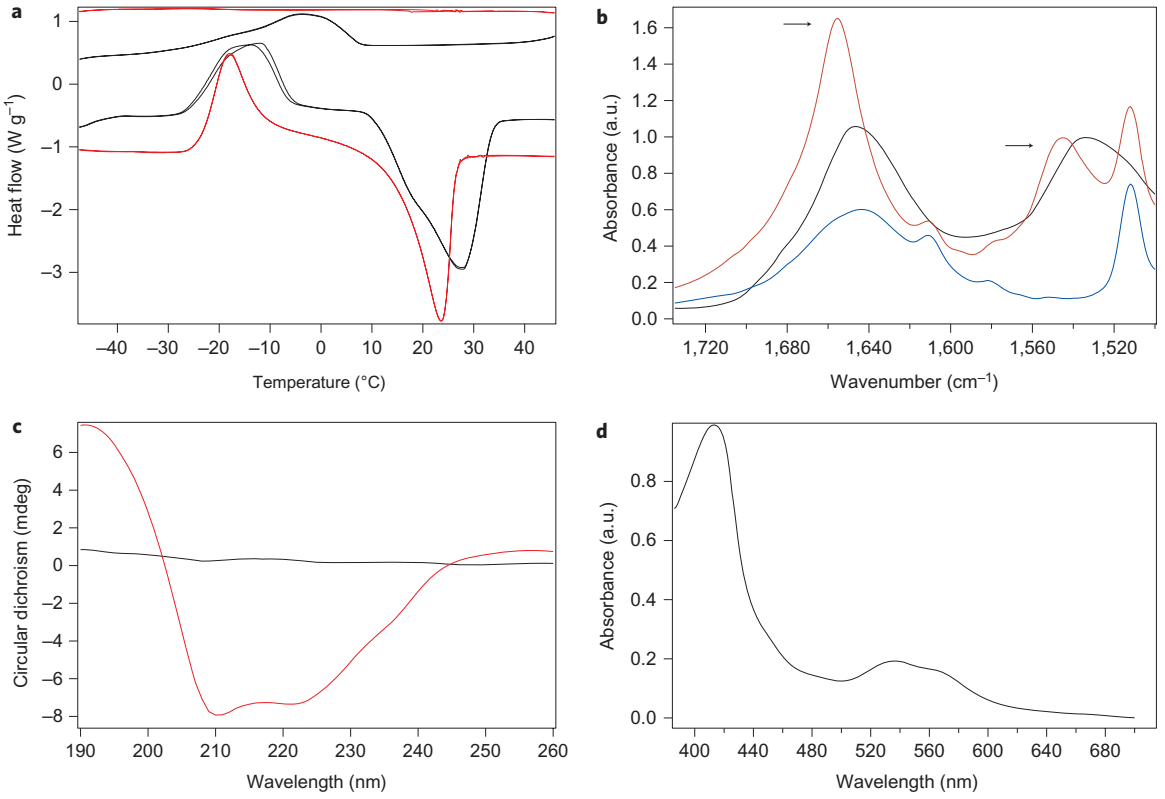

Figure 2 | Characterization of solvent-free [C–Mb][S_1] nanoconstructs and melts. a, DSC traces for the polymer surfactant S_1 (black line) and [**C**–Mb][S_1] solvent-free nanoconstruct (red line) showing their melting transitions at 27.5 and 23.5 °C, respectively. The isothermal cycles show complete reversibility, with no detectable thermal hysteresis. **b**, ATR-FTIR spectra of lyophilized Mb (black line), [**C**-Mb][S_1] solvent-less liquid (red line) and S_1 (blue line). Arrows indicate the positions of the amide I (1,655 cm^{-1}) and amide II (1,545 cm^{-1}) bands. **c**, Far-UV CD spectra of S_1 (black line) and [**C**-Mb][S_1] melt showing minima at 208 and 222 nm. **d**, Diffuse reflectance UV–Vis spectrum of a [**C**-Mb][S_1] melt at 25 °C, showing a Soret band at 413 nm and Q_α and Q_β bands at 564 and 536 nm, respectively.

shoulder at 18 °C and a minimum at 27.5 °C, in contrast to a single melting transition at 23.5 °C for [**C**–Mb][S_1]. Collapse of the two-stage melting transition indicated coupling between the melting events of the hydrocarbon and polyethylene chains in [**C**–Mb][S_1], and hence an increase in cooperativity between these structural domains in the electrostatically coupled polymer surfactant.

Spectroscopic studies were undertaken to determine the nature of the protein secondary structure associated with the [**C**–Mb][S_1] and [**C**–Mb][S_2] melts. Significantly, attenuated total reflectance-Fourier transform infrared (ATR–FTIR) experiments showed that the cationized protein retained its near-native secondary structure in the solvent-less liquid phase (Fig. 2b). The spectrum of the [**C**–Mb][S_1] melt shows symmetrical amide I and II bands centred at 1,655 cm^{-1} and 1,544 cm^{-1}, respectively, with an amide I:II peak intensity ratio of 1.7, as well as strong absorbances at 1,512, 1,580 and 1,610 cm^{-1} that correspond to the aromatic C–C stretches of the para-substituted phenyl moiety. The position of the amide I and II bands and their relative intensities are consistent with protein molecules containing predominately α-helical structure[17,18]. In contrast, the amide I band of pure lyophilized Mb was shifted to a lower wavenumber (1,648 cm^{-1}) and had a lower amide I:II peak intensity ratio, which suggested an increased level of random coil (1,640–1,651 cm^{-1}) or β-sheet formation (1,626–1,640 cm^{-1})[19].

In addition, circular dichroism (CD) spectra from the [**C**–Mb][S_1] melt show peaks at 208 and 222 nm, consistent with a significant degree of α-helical secondary structure (Fig. 2c). Comparison of the peak intensity ratio ($R = I_{208}/I_{222}$) for the CD spectra recorded for aqueous native Mb, aqueous **C**–Mb, aqueous [**C**–Mb][S_1], a [**C**–Mb][S_1] melt and a [**C**–Mb][S_1] melt after re-dissolution in water gave values of 0.9, 1.2, 1.1, 1.0 and 1.2, respectively (Supplementary Fig. S6), indicating only small changes in the folded structure associated with the native aqueous protein and solvent-free [**C**–Mb][S_1] nanoconstruct. Persistence of the near-native protein structure in the solvent-free met-[**C**–Mb][S_1] liquid was also supported by diffuse reflectance UV–Vis spectroscopy, which showed a strong Soret band at 413 nm, as well as Q_α and Q_β bands at 564 and 536 nm, respectively (Fig. 2d). The three absorption bands were indicative of a haem prosthetic group with six-coordinate geometry, although the Soret band was redshifted and the Q_α band blueshifted relative to aqueous met-Mb (Soret = 408 nm; Q_α = 620 nm)[20], which suggests a low-spin complex with a strongly bound water molecule[21]. A similar geometry was also observed for aqueous solutions of cationized met-Mb, which exhibited a redshifted Soret band (411 nm) (Supplementary Fig. S7), suggesting that the global increase in the charge density produces a significant enhancement in the dielectric constant associated with the distal haem pocket.

Given the high level of secondary and tertiary structure associated with the solvent-less [**C**–Mb][S_1] liquids, we were confident that the protein melts should exhibit aspects of biomolecular functionality under appropriate experimental conditions. As a proof of principle, we prepared aqueous deoxy-[**C**–Mb][S_1] nanoconjugates by first reducing the met-[**C**–Mb][S_1] nanoconstruct under anaerobic conditions in the presence of aqueous Na_2S, followed by quenching in liquid nitrogen before lyophilization and thermally induced melting (see Supplementary Materials and Methods). UV–Vis spectra of the resulting solvent-free fluid showed a well-defined Soret band at 424 nm, as well as a strong Q_α band at 555 nm and a weaker Q_β band at 527 nm (Fig. 3a), consistent with the formation

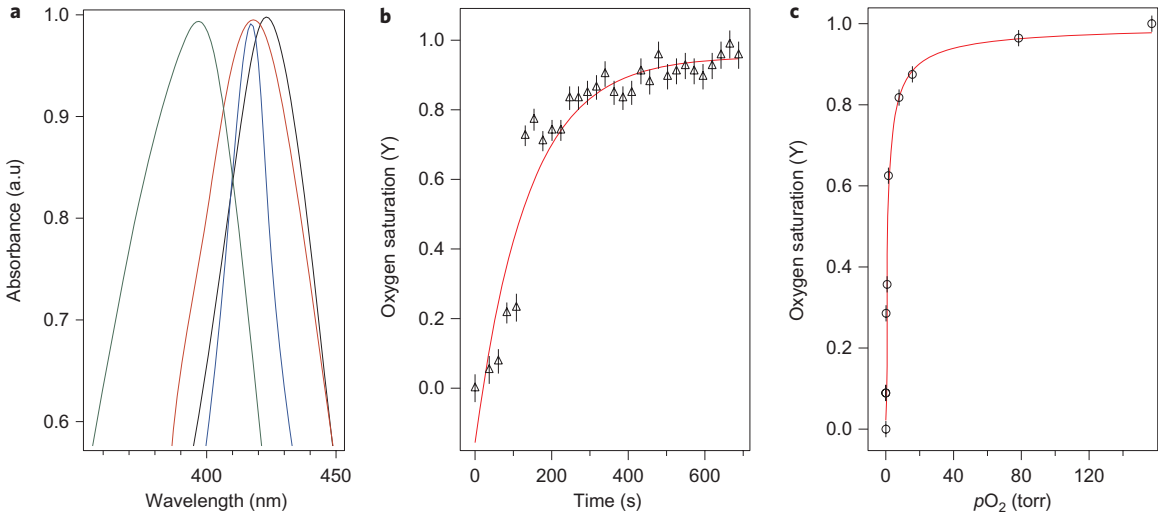

Figure 3 | Gas molecule binding to solvent-free [C–Mb][S_1] liquids at room temperature. a, Diffuse reflectance UV–Vis spectra showing associated shifts in the Soret band for deoxy-[**C**–Mb][$\mathbf{S}_1$] (black line), oxy-[**C**–Mb][$\mathbf{S}_1$] (red line), CO–[**C**–Mb][$\mathbf{S}_1$] (blue line) and SO_2–[**C**–Mb][$\mathbf{S}_1$] (green line). Spectra over an extended wavelength range are presented in Supplementary Fig. S8. **b**, Plot of degree of oxygen saturation with time showing the rate of dioxygen binding to a deoxy-[**C**–Mb][$\mathbf{S}_1$] melt at 37 °C. Data points (triangles) originate from Gaussian fits to the Soret band, and were fitted using an exponential decay function (red line). **c**, Equilibrium dioxygen association curve showing degree of oxygen saturation against partial pressure of dioxygen (pO_2) for [**C**–Mb][$\mathbf{S}_1$] at 37 °C. Data points (triangles) originate from Gaussian fits to the Soret band, and were fitted using the Hill equation (red line). Error bars in **b** and **c** result from fitting of Gaussian functions to the Soret bands and represent a total width of two standard deviations.

of a deoxygenated Fe(II) porphyrin metallocentre in the melt phase. Significantly, exposure of the deoxy-[**C**–Mb][$\mathbf{S}_1$] melt to dioxygen in a dry environment resulted in a shift in the Soret band to 418 nm, signifying uptake and binding of dioxygen to the haem group of protein molecules present in the solvent-free state (Fig. 3a; see also Supplementary Fig S8). CO binding to the deoxymyoglobin melt was also indicated by a shift in the Soret band to 417 nm (Fig. 3a). Moreover, exposure of the met-[**C**–Mb][$\mathbf{S}_1$] melt to gaseous SO_2 produced a shift in the Soret and Q-bands to values of 396 and 635 nm, respectively, indicating that the ligated water molecule in the distal haem pocket was displaced by SO_2 binding at the metallocentre (Fig. 3a). The presence of bound SO_2 was confirmed by ATR–FTIR spectroscopy, which showed a characteristic absorbance at 1,330 cm^{-1} (Supplementary Fig. S9).

Significantly, in each case, binding of the gas molecules was reversible such that dissociation of the ligands was readily achieved by placing the Mb melts under vacuum. This procedure was used to develop an equilibrium binding assay to quantitatively assess the dioxygen binding efficiency of the solvent-free liquids. To ensure that measurements were made at equilibrium, dioxygen-binding rate experiments were conducted on the solvent-free protein liquids by monitoring the changing position of the Soret band at atmospheric pressure and 37 °C. In this way, the rate of dioxygen binding to the deoxy-[**C**–Mb][$\mathbf{S}_1$] melt was approximated to an exponential decay function (Fig. 3b). Notably, the reaction timescales were of the order of minutes rather than milliseconds (as observed for O_2 binding to deoxy-Mb in aqueous media[22]) due to constraints on the rate of dioxygen diffusion though the viscous [**C**–Mb][$\mathbf{S}_1$] fluid. Indeed, equilibrium values for a given partial pressure of dioxygen were only reached after ~10 min. This was consistent with the viscosity of the melts (1.7×10^3 Pa s), which gave an estimated diffusion time of 17 min for a sample thickness of 2 μm. Significantly, Fig. 3c shows the equilibrium dioxygen association curve for a [**C**–Mb][$\mathbf{S}_1$] melt at 37 °C, where each data point was generated from a Gaussian fit to the Soret band at a given partial pressure of oxygen. The data were fitted using the Hill equation (see Supplementary Materials and Methods), and gave a Hill coefficient of 0.8, which indicates independent binding and hence no evidence of cooperativity. The value for the oxygen affinity ($P_{1/2}$) was 1.1 torr, which is in good agreement with dioxygen binding studies on equine heart Mb under physiological conditions[23].

In conclusion, we have shown the unprecedented formation, at room temperature and pressure, of solvent-free protein liquids of a haem metalloprotein by the melting of single-component, stoichiometric myoglobin–polymer surfactant nanoconstructs. The Mb-containing melts comprised solvent-free protein molecules that exhibited near-native structures and retained their ability to reversibly bind dioxygen and other gaseous ligands. Diffusional constraints associated with the viscosity of the solvent-less protein liquids markedly reduced the rate of ligand binding, although the melts exhibited classical equilibrium binding curves, suggesting that they could be used as novel biomolecule-based functional fluids.

The persistence of structure and function in the Mb-containing melts can be reconciled with the presence of 20 PEO units associated with the anionic polymer surfactant $\mathbf{S}_1$, as it is well documented that surfactants comprising alkyl chains alone (such as sodium dodecyl sulfate) actively promote protein denaturation[24,25]. Polymer surfactant conjugation to cationized myoglobin gave rise to only a 1.5 nm increase in the hydrodynamic diameter, which was commensurate with a coronal layer containing surfactant molecules arranged in a compact conformation[26]. As a consequence, on removal of the solvent and heating of the ionic nanoconstructs, the PEO chains facilitate the dissipation of thermal energy through conformational changes associated with their dynamical freedom. Melting is then achieved if the PEO chains are sufficiently extended to sustain long-range attractive interactions between the thermally activated molecules (in the case of the [**C**–Mb][$\mathbf{S}_2$] constructs this required a minimum of 11 PEO units per polymer surfactant molecule). To a degree, this soft, flexible coronal layer is analogous to the entrapped water shell that persists on the surface of proteins in nonpolar solvents, and which elicits enzyme function. Although the presence of tightly bound structural water molecules in the Mb-containing solvent-free liquids cannot be discounted—indeed the UV–Vis spectra of the met-[**C**–Mb][$\mathbf{S}_1$] melts were consistent with a strongly bound water molecule in the distal

haem pocket—a hydrated structural shell around the molten protein would not be stabilized by the polymer surfactant due to its inherently high water solubility. Moreover, such a layer would be unlikely to remain at temperatures as high as 250 °C, where no significant mass losses were observed during thermogravimetric analysis of the liquid myoglobins. Thus, it is possible that the structure and binding ability of the polymer surfactant–myoglobin nanoconjugates could be maintained in the liquid phase in the absence of a structural ensemble of solvent molecules. These new types of biohybrid nanoconstructs could therefore present a significant challenge to existing theories on the role of water molecules in determining protein structure and function.

Methods

Protein cationization. Coupling of DMPA to aspartic and glutamic acid residues on the external surface of met-Mb was undertaken using carbodiimide activation. Solutions of DMPA were adjusted to pH 6 using 6 M HCl, and were added dropwise to a stirred protein solution. The coupling reaction was initiated by adding *N*-(3-dimethylaminopropyl)-*N*′-ethylcarbodiimide hydrochloride (EDC) immediately. The pH was maintained using dilute HCl, and solutions were stirred for 12 h. The solutions were then centrifuged to remove any precipitate and the supernatant was dialysed (Visking dialysis tubing, 7 kDa molecular weight cut-off (MWCO)) extensively against high-purity water to produce stable solutions of the DMPA-cationized protein, **C**–Mb.

Protein–polymer surfactant nanoconjugates. Complexation of the anionic polymer surfactants $\mathbf{S}_1$, $\mathbf{S}_2$, $\mathbf{S}_3$ or $\mathbf{S}_4$ to **C**–Mb was undertaken by adding an aqueous solution of the cationized protein (4 mg ml^{-1}) to a stirred viscous liquid of the pure surfactant to give a protein:surfactant ratio of 1:3 wt/wt. The solution was then stirred for 12 h and centrifuged to remove any precipitate, and the supernatant was dialysed (Visking dialysis tubing 7 kDa MWCO) extensively against Milli-Q quality water for 48 h to produce aqueous solutions of the nanoconjugates, designated as [**C**–Mb][$\mathbf{S}_x$] ($x = 1$–4).

Protein melts. Aqueous samples of the protein–surfactant nanoconjugates were lyophilized for 48 h and the resulting nanostructured ionic solids were stored in a desiccator under vacuum. Solvent-free protein melts were prepared by heating the lyophilized/desiccated protein–surfactant nanoconjugates to temperatures of ~40 °C to produce clear viscous liquids of [**C**–Mb][$\mathbf{S}_x$] ($\mathbf{S}_x = \mathbf{S}_1$ or $\mathbf{S}_2$). Deoxy-Mb-containing nanoconjugates were produced by dialysing cationized met-Mb exhaustively against degassed Milli-Q water containing 0.06 M $Na_2S_2O_4$ for 24 h under a continuous nitrogen purge. After complexation of deoxy-[**C**–Mb] with surfactant ($\mathbf{S}_1$), the resultant conjugates were dialysed against degassed Milli-Q water containing 0.08 M Na_2S under a nitrogen atmosphere for 24 h. The solution was then lyophilized for 48 h and heated to 60 °C in a dry environment under nitrogen to yield the corresponding deoxy-[**C**–Mb][$\mathbf{S}_1$] melt. The resultant material was stored in a sealed vial under a dry nitrogen atmosphere.

Ligand binding assays. Ligand binding experiments were undertaken by first applying a film of the deoxy-[**C**–Mb][$\mathbf{S}_1$] to the inside of a glass tube fitted with a Youngs tap under a nitrogen environment. For SO_2 and CO binding studies, the modified Youngs tube was placed under vacuum overnight, and then connected to the corresponding cylinder and exposed to the appropriate gas. For SO_2 the pressure was controlled by means of an oil bubbler, and for the CO experiment the sample was exposed to 1.5 bar of CO. For O_2 kinetic and equilibrium experiments, a purpose-built pressure apparatus was assembled, allowing accurate control of the partial pressures of O_2, which were measured using an interfaced Pirani gauge.

Further details of solvent-free myoglobin synthesis and characterization techniques, as well as associated references, are given in the Supplementary Information.

Received 18 February 2010; accepted 12 May 2010; published online 6 June 2010

References

1. Rariy, R. V. & Klibanov, A. M. Correct protein folding in glycerol. *Proc. Natl Acad. Sci. USA* **94,** 13520–13523 (1997).
2. Knubovets, T., Osterhout, J. J., Connolly, P. J. & Klibanov, A. M. Structure, thermostability, and conformational flexibility of hen egg-white lysozyme dissolved in glycerol. *Proc. Natl Acad. Sci. USA* **96,** 1262–1267 (1999).
3. Clark, D. S. Characteristics of nearly dry enzymes in organic solvents: implications for biocatalysis in the absence of water. *Phil. Trans. R. Soc. Lond. B* **359,** 1299–1307 (2004).
4. van Rantwijk, F. & Sheldon, R. A. Biocatalysis in ionic liquids. *Chem. Rev.* **107,** 2757–2785 (2007).
5. Kikkawa, S., Takahashi, K., Katada, T. & Inada, Y. Esterification of chiral secondary alcohols with fatty-acid in organic-solvents by polyethylene glycol-modified lipase. *Biochem. Int.* **19,** 1125–1131 (1989).
6. Kodera, Y., Nishimura, H., Matsushima, A., Hiroto, M. & Inada, Y. Lipase made active in hydrophobic media by coupling with polyethylene-glycol. *J. Am. Oil Chem. Soc.* **71,** 335–338 (1994).
7. Basri, M. *et al.* Synthesis of fatty esters by polyethylene glycol-modified lipase. *J. Chem. Technol. Biot.* **64,** 10–16 (1995).
8. Okahata, Y. & Ijiro, K. A lipid-coated lipase as a new catalyst for triglyceride synthesis in organic solvents. *Chem. Commun.* 1392–1394 (1988).
9. Okahata, Y. & Ijiro, K. Preparation of a lipid-coated lipase and catalysis of glyceride ester syntheses in homogeneous organic solvents. *Bull. Chem. Soc. Jpn* **65,** 2411–2420 (1992).
10. Mattos, C. & Ringe, D. Proteins in organic solvents. *Curr. Opin. Struct. Biol.* **11,** 761–764 (2001).
11. Liu, L., Bagal, D., Kitova, E. N., Schnier, P. D. & Klassen, J. S. Hydrophobic protein–ligand interactions preserved in the gas phase. *J. Am. Chem. Soc.* **131,** 15980–15981 (2009).
12. Perriman, A. W., Colfen, H., Hughes, R. W., Barrie, C. L. & Mann, S. Solvent-free protein liquids and liquid crystals. *Angew. Chem. Int. Ed.* **48,** 6242–6246 (2009).
13. Lin, Y. *et al.* Self-directed self-assembly of nanoparticle/copolymer mixtures. *Nature* **434,** 55–59 (2005).
14. Wong, K. K. W. & Mann, S. Biomimetic synthesis of cadmium sulphide–ferritin nanocomposites. *Adv. Mater.* **8,** 928–932 (1996).
15. Costantino, H. R., Curley, J. G. & Hsu, C. C. Determining the water sorption monolayer of lyophilized pharmaceutical proteins. *J. Pharm. Sci.* **82,** 1390–1393 (1997).
16. Pauling, L. The adsorption of water by proteins. *J. Am. Chem. Soc.* **67,** 555–557 (1945)
17. Goormaghtigh, E., Ruysschaert, J. M. & Raussens, V. Evaluation of the information content in infrared spectra for protein secondary structure determination. *Biophys. J.* **90,** 2946–2957 (2006).
18. Ishida, K. P. & Griffiths, P. R. Comparison of the amide-I/II intensity ratio of solution and solid-state proteins sampled by transmission, attenuated total reflectance, and diffuse reflectance spectrometry. *Appl. Spectrosc.* **47,** 584–589 (1993).
19. Pelton, J. T. & McLean, L. R. Spectroscopic methods for analysis of protein secondary structure. *Anal. Biochem.* **277,** 167–176 (2000).
20. Li, Q. C. & Mabrouk, P. A. Spectroscopic and electrochemical studies of horse myoglobin in dimethyl sulfoxide. *Phil. Trans. R. Soc. Lond. B* **8,** 83–94 (2003).
21. Ikedasaito, M. *et al.* Coordination structure of the ferric heme iron in engineered distal histidine myoglobin mutants. *J. Biol. Chem.* **267,** 22843–22852 (1992).
22. Antonini, E. & Brunori, M. Hemoglobin and myoglobin in their reactions with ligands (eds Neuberger, A. & Tatum, E. L.) (North Holland Publishing Company, 1971).
23. Schenkman, K. A., Marble, D. R., Burns, D. H. & Feigl, E. O. Myoglobin oxygen dissociation by multiwavelength spectroscopy. *J. Appl. Physiol.* **82,** 86–92 (1997).
24. Andersen, K. K., Westh, P. & Otzen, D. E. Global study of myoglobin–surfactant interactions. *Langmuir* **24,** 399–407 (2008).
25. Andersen, K. K. *et al.* The role of decorated SDS micelles in sub-CMC protein denaturation and association. *J. Mol. Biol.* **391,** 207–226 (2009).
26. Lee, H., de Vries, A. H., Marrink, S. J. & Pastor, R. W. A coarse-grained model for polyethylene oxide and polyethylene glycol: conformation and hydrodynamics. *J. Phys. Chem. B* **113,** 13186–13194 (2009).

Acknowledgements

We thank EPSRC (Platform grant no. EP/C518748/1) for financial support, A. Völkel for performing the analytical ultracentrifugation experiments, and J. Lewis for performing the high-speed macro photography.

Author contributions

S.M. and A.W.P. contributed to the project's inception. A.P.S.B. and A.W.P. designed the experiments and performed the synthesis. H.C. performed the analysis on the analytical ultracentrifugation results, N.T., G.R.O., A.P.S.B. and A.W.P. conducted the ligand binding studies, and S.M. and A.W.P. wrote the paper. All authors discussed the results and commented on the manuscript.

Additional information

The authors declare no competing financial interests. Supplementary information accompanies this paper at www.nature.com/naturechemistry. Reprints and permission information is available online at http://npg.nature.com/reprintsandpermissions/. Correspondence and requests for materials should be addressed to S.M.